



ELSEVIER

Contents lists available at ScienceDirect

Applied Radiation and Isotopes

journal homepage: www.elsevier.com/locate/apradiso

The optimization of an energy-dispersive X-ray diffraction system for potential clinical application

A. Chaparian^{a,*}, M.A. Oghabian^b, V. Changizi^c, M.J. Farquharson^d

^a Shahid Sadoughi University of Medical Sciences, Department of Medical Physics, PhD, Yazd, Iran

^b Tehran University of Medical Sciences, Department of Medical Physics, PhD, Tehran, Iran

^c Tehran University of Medical Sciences, Department of Radiology Technology, PhD, Tehran, Iran

^d McMaster University, Department of Medical Physics and Applied Radiation Sciences, Ontario, Canada

ARTICLE INFO

Article history:

Received 20 April 2010

Received in revised form

1 June 2010

Accepted 7 July 2010

Keywords:

EDXRD

Optimization

Sensitivity

Spatial resolution

Momentum transfer resolution

Clinical application

ABSTRACT

In the past decade, energy-dispersive X-ray diffraction (EDXRD) has been used to identify the nature of tissues. However, these systems have limited clinical use because of problems such as the long measurement times. In this study, the relation between various setup parameters and some performance specifications such as sensitivity, spatial resolution and momentum transfer resolution were assessed using both geometrical calculations and modeling. Accuracy of the derived relations was also confirmed by means of experimental measurements. As an example, the optimum parameters were determined for obtaining diffraction patterns of breast tissue for an efficient acquisition time. Accordingly, the results of this study could introduce a useful tool for EDXRD optimization in clinical application.

© 2010 Elsevier Ltd. All rights reserved.

1. Introduction

It has been shown that X-ray coherent scatter from biological tissues can give information about the characteristics of tissue and enhance conventional transmission imaging.

This information is obtained via constructive interference of coherent scatter with biological tissues and presented as individual diffraction patterns. Many scientists have shown that coherent scattering could be used for biological tissues' characterization (Speller, 1999; Poletti et al., 2002; Cunha et al., 2006; Chaparian et al., 2009). These studies have distinguished normal and cancerous tissue using the diffraction patterns resulting from coherent scatter. These diffraction patterns are usually expressed as a function of the momentum transfer argument (χ),

$$\chi = (E/hc)\sin(\theta/2) \quad (1)$$

where E is the photon energy, h the Planck's constant, c the speed of light and θ the angle of scatter. The diffraction patterns show differences that could be important in the determination of tissue types; peak position and full-width at half-maximum (FWHM) are two such parameters that can be utilized to differentiate between tissues.

There are two basic methods for obtaining diffraction patterns from materials; namely angular-dispersive X-ray diffraction (ADXRD) and energy-dispersive X-ray diffraction (EDXRD). In ADXRD the diffraction pattern is obtained by using monoenergetic photons and recording the angular distribution of scattered photons. Alternatively, EDXRD is based on using a polyenergetic photon spectrum obtained from a conventional X-ray tube. In such a system, scatter intensity is recorded at a fixed scatter angle by an energy-resolving detector (e.g. HPGe) (Theodorakou and Farquharson, 2008).

The EDXRD system satisfies all of the characteristics required to study the properties of tissues, but the system is not yet suitable for clinical usage. The need for long measurement times and hence high dose, seems to be the most important problem of this system. Kidane et al. (1999), LeClair et al. (2006), Farquharson and Geraki (2004) and Changizi et al. (2005); Changizi et al. (2008) used an EDXRD method for breast tissue characterization with a measurement time of 500–600 s per sample.

This study focuses on the optimization of an EDXRD system in order to maximize the detection sensitivity for a potential clinical usage. The idea comes from the fact that diffraction patterns of amorphous materials, such as biological tissues, are circularly symmetric around the primary beam; therefore using a circular slit collimator considerably enhances the sensitivity of scatter detection. However, three basic features of the EDXRD system namely sensitivity, spatial resolution and momentum transfer

* Corresponding author.

E-mail address: chaparian@ssu.ac.ir (A. Chaparian).

resolution are highly interrelated and therefore may not be considered individually. Since all experimental methods of optimization are time-consuming and expensive, computational methods are usually preferred.

LeClair et al. (2006) used EDXRD measurements coupled with a semianalytical model to extract the differential linear scattering coefficients of breast tissues on absolute scales. Their technique was validated using a 50 kV polychromatic X-ray beam incident on a sample of water. The sample to detector distance was 29 cm and the duration of each measurement was 10 min.

Bomsdorf et al. (2004) presented quantitative simulation as a means for system optimization and evaluated possible photon scatter paths using a Monte Carlo algorithm. They also gave examples on materials such as Al/SiC-composite to illustrate how system performance for a given experimental situation may be optimized by means of the simulation program.

The aim of our study was to define relations between different setup parameters of an EDXRD system. The aim was to determine the optimal parameters for an improved detection sensitivity of the system, taking into account acceptable levels of spatial and momentum transfer resolution for clinical applications.

2. Materials and methods

2.1. Setting up the EDXRD system

A setup including an X-ray tube, two primary collimator diaphragms, the scatter collimator diaphragms and HPGe detector was considered (Fig. 1).

The primary collimator defines an X-ray pencil beam incident on the tissue sample. The photons scattered under a pre-defined scatter angle are collected by means of a rotationally symmetric scatter collimator consisting of two ring diaphragms of different diameters. The scatter angle (θ) can be set by moving the upper diaphragm of the collimator in the vertical direction or by changing the radius of diaphragms.

The primary collimator is composed of two parallel planes having a hole in the center, which are located at a certain distance from each other. The distance between the two planes specifies the primary collimator length (PCL) and the diameter of the holes specifies the primary collimator diameter (PCD). The width of the beam emerging from this collimator specifies the horizontal dimension of the region of interest (HROI).

The main parameters of the scatter collimator include the width of the upper diaphragm (W_{s1}), width of the lower diaphragm (W_{s2}), radius of the upper diaphragm (R_1), radius of the lower diaphragm (R_2), the scatter collimator length (SCL), leaf thickness of the collimator (LT), sample to detector distance (SDD) and scatter angle (θ) (Fig. 2).

Scatter angle (θ) is calculated by the following relation:

$$\theta = \tan^{-1} \left(\frac{R_2 + \frac{W_{s2}}{2} - R_1 - \frac{W_{s1}}{2}}{SCL} \right) \quad (2)$$

Sample to detector distance (SDD) is also defined as

$$SDD = \frac{R_2 + \frac{W_{s2}}{2}}{\tan \theta} \quad (3)$$

With a fixed R_2 , this distance is mainly dependent on the scatter angle (θ).

2.2. Optimization of the EDXRD system

Initially, we derived the relationship between different parameters of the system and its resultant spatial resolution, momentum transfer resolution and sensitivity by means of

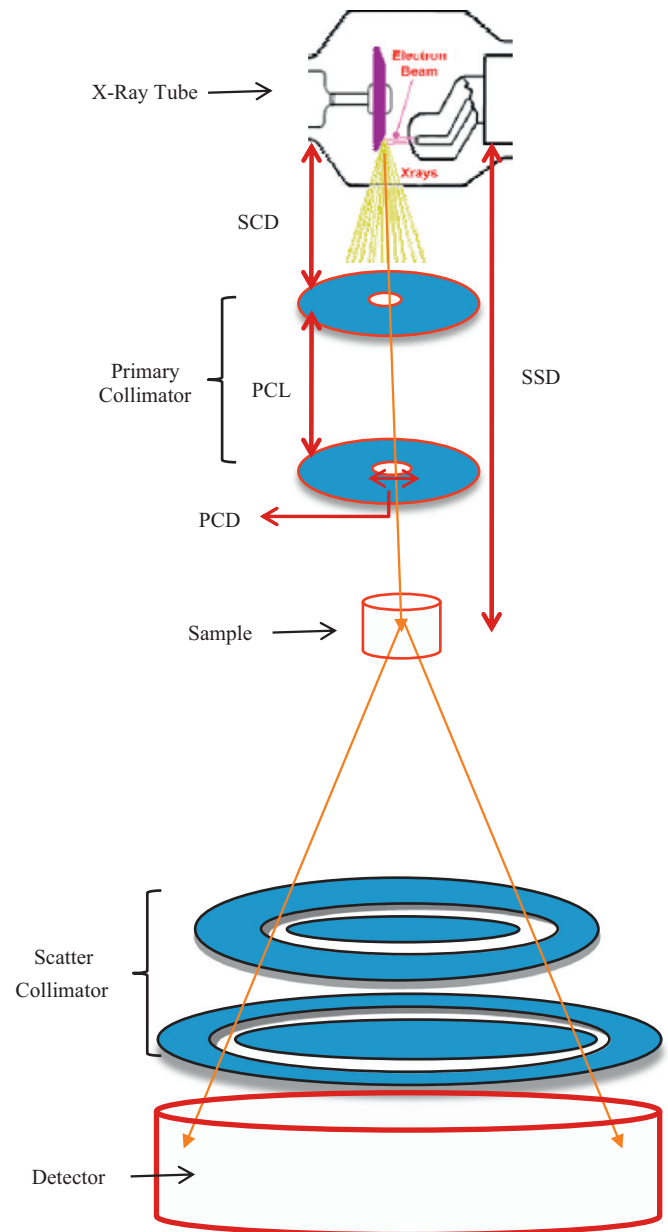


Fig. 1. Schematic view of the general setup of the EDXRD system (not to scale).

geometrical calculations. In the second step, the accuracy of the derived relations was validated by experimental tests. Finally, having considered an acceptable level for spatial and momentum transfer resolution, setting up parameters were determined for each type of application and tissue type, in regard to increasing the sensitivity.

2.2.1. Derivation of the relationship between system parameters and spatial resolution

The dimension of the horizontal region of interest (HROI), which depends on the width of the primary beam in the center of the tissue of interest is a criterion of horizontal spatial resolution. We derived the following equation showing the relation between geometrical parameters and HROI as shown in Fig. 1:

$$HROI = \frac{(PCD \times SDD) + (a(SDD - (SCD + PCL)))}{SCD + PCL} \quad (4)$$

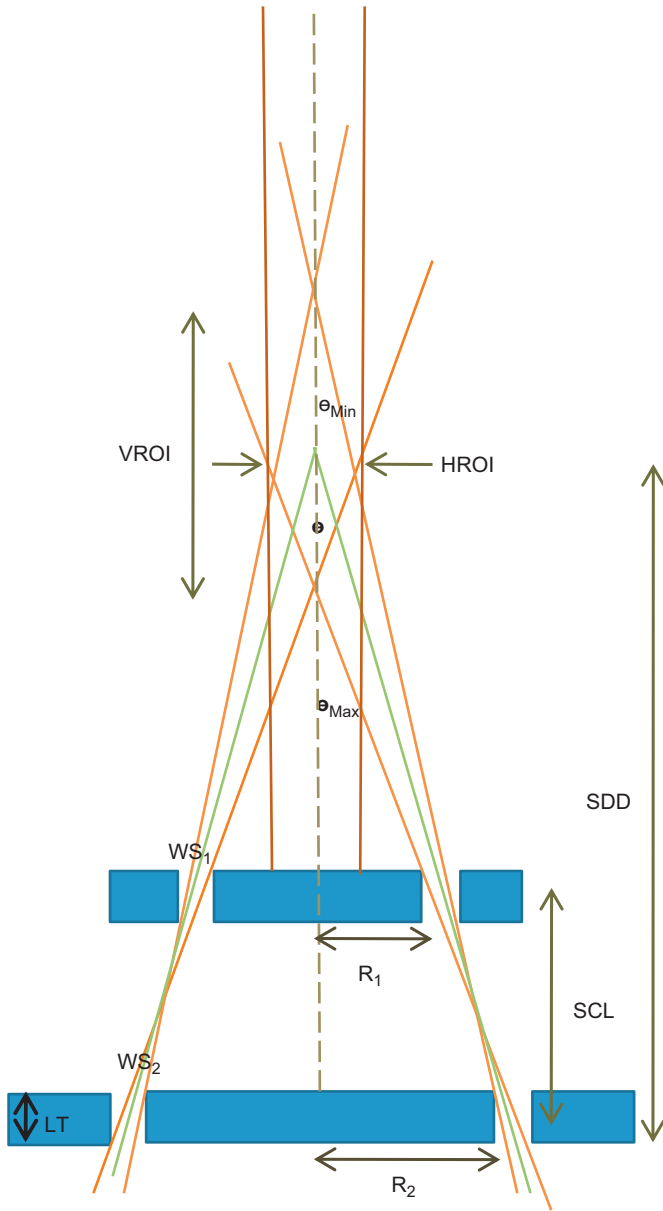


Fig. 2. Vertical view of the scatter collimator and the region of interest (drawing not true to scale).

where SSD is the source to sample distance, α the focal spot size, SCD the source to collimator distance. As illustrated in this equation, the HROI, and thus horizontal spatial resolution is dependent mainly on the primary collimator parameters and the SSD but it is independent of the scatter collimator parameters.

On the other hand, the vertical spatial resolution depends on the VROI as shown in Fig. 2. The VROI can be derived geometrically by the following relation:

$$VROI = \frac{(R_1 + WS_1)(SCL - LT)}{(R_2 - R_1 - WS_1)} - \frac{R_1(SCL + LT)}{(R_2 - R_1 + WS_2)} \quad (5)$$

It is noticeable that the VROI and thus vertical spatial resolution are mainly determined by the scatter collimator characteristics.

2.2.2. Derivation of the relationship between system parameters and momentum transfer resolution

To differentiate among diffraction patterns of different tissues, a suitable momentum transfer resolution (MR) is required. In low

MR, the FWHM of the diffraction pattern curve will be increased and therefore adjacent peaks may overlap and this makes detection harder.

The two main sources of momentum blurring (MB) are the angular blurring (AB) and the energy blurring (EB) of the detector. The MB of the system is a measure of MR, given by the following relation:

$$MB = \sqrt{(AB)^2 + (EB)^2} \quad (6)$$

where the AB represents the angular range over which scatter beam is incident on the detector and the EB the characteristic of the detector system, which is introduced as energy resolution. Energy blurring for the cooled HpGe detector used in this study is in the order of 0.49 keV at 59.5 keV; leading to a momentum transfer blurring value of about 0.8%. Therefore, AB is the most significant source of momentum transfer blurring. AB as a criterion of angular resolution can be obtained geometrically by

$$AB = \frac{\sin\left(\frac{\theta + \Delta\theta}{2}\right) - \sin\left(\frac{\theta}{2}\right)}{\sin\left(\frac{\theta}{2}\right)} \quad (7)$$

where

$$\Delta\theta = \frac{\theta_{max} - \theta_{min}}{2} \quad (8)$$

Referring to Fig. 2, θ_{max} and θ_{min} can be obtained using the following relations:

$$\theta_{max} = \tan^{-1}\left(\frac{R_2 + WS_2}{SDD - \left(\frac{VROA}{2}\right)}\right) \quad (9)$$

$$\theta_{min} = \tan^{-1}\left(\frac{R_2}{SDD + \left(\frac{VROA}{2}\right) - LT}\right) \quad (10)$$

For a certain detector at a fixed angle, the MR is mainly affected by the changing of Ws and SCL.

2.2.3. Derivation of the relationship between system parameters and sensitivity

The sensitivity is important because it contributes to the amount of measurement time needed. In a high sensitivity system, recording a diffraction pattern with definite peak height needs shorter measurement time in comparison with a low sensitivity system.

Both primary and scatter collimator parameters determine the volume of interest (i.e. volume of scattering) (Vs) within the tissue. It is clear that an increase in Vs, leads to an increase in sensitivity since more scattered photons can reach the detector. Therefore finding a relation between collimator parameters and Vs helps to optimize the sensitivity. The following equation has been derived between the geometrical parameters and Vs based on Figs. 1 and 2:

$$V_s = \frac{\pi}{4} \left[\frac{(R_1 + WS_1)(SCL - LT)}{(R_2 - R_1 - WS_1)} - \frac{R_1(SCL + LT)}{(R_2 - R_1 + WS_2)} \right] \left[\frac{(PCD \times SSD) + (\alpha(SSD - (SCD + PCL)))^2}{SCD + PCL} \right]^2 \quad (11)$$

Considering relations 4 and 5, this relation can be simplified as

$$V_s = \frac{\pi}{4} (VROI)(HROI)^2 \quad (12)$$

However, the time of measurement is also proportional to other parameters such as the output of the X-ray tube and the efficiency of the detector. Whilst the output of the X-ray tube and the efficiency of the detector should be chosen as high as possible in order to decrease the measurement time, the role of the collimator dimensions is more difficult to evaluate.

2.2.4. Derivation of the relationship between scatter angle (θ) and incident photon energy

The angles of the scattered photons and incident photon energy are important parameters in the EDXRD system because these parameters determine the momentum transfer range of the resultant diffraction pattern (Eq. (1)).

As mentioned, in an EDXRD system with a polyenergetic source, the measurement at a suitable angle would be sufficient to record a diffraction pattern in the entire available momentum transfer (χ) range. In fact, any other measurement at a smaller angle would produce an incomplete diffraction pattern. For example, the peak positions of water and adipose in corresponding diffraction patterns are located at 1.6 and 1.1 nm⁻¹, respectively. However, it is necessary for preserving the whole pattern of these materials to include the momentum transfer up to 3.17 and 2.45 nm⁻¹, respectively. We call these values as minimum acceptable momentum transfer ($\chi_{m.a}$). Then the minimum acceptable angle ($\theta_{m.a}$) can be calculated by

$$\theta_{m.a} = 2 \sin^{-1} \left(\frac{\chi_{m.a} hc}{E_{max}} \right) \quad (13)$$

where E_{max} is the maximum energy of the X-ray incident spectrum (for example 50 kVp). On the other hand, using large angles induces degradation of the diffraction pattern because of Compton scattering. Therefore selecting a suitable angle is very important for optimization process.

2.2.5. Experimental setup for validation of computational methods

After obtaining the optimum parameters for our setup by means of geometrical calculations, it was necessary to validate this computational method by experimental measurements. Firstly we designed and built a flexible system constituting primary and scatter collimators and a sample holder (Fig. 3).

The system incorporates a moveable frame and five holders, which can adjust various geometric parameters between the collimators and the detecting system. The source was a tungsten target conventional X-ray tube which can operate at 50 kVp and 10 mA. The scattered photons were detected using a high purity germanium detector with a planar crystal of radius 22 mm and

thickness of 15 mm (model GPD 50/400 Ortec). This detector has an energy resolution of 0.49 keV at 59.5 keV. Initially, diffraction patterns from water were recorded in different situations in order to test the system. It is necessary to correct the raw spectrum for several effects including background radiation, the non-uniform intensity spectrum of the incident beam, multiple scatter and the attenuation of primary and scatter radiation. When the sample is relatively small in the range of some millimeters, only the first two corrections are important. The last two corrections were also ignored for the small samples in the previous studies such as the Harding's study (Harding et al., 1990). After subtracting the background spectrum, the diffraction patterns were normalized to the intensity of the incident beam.

The peak height of the resultant diffraction pattern was used for the evaluation of sensitivity. The FWHM of the main peak is a measure of the MB or MR experimentally. A system with better MR will have a narrower peak and therefore smaller FWHM. In this regard, FWHM is only used for a pure crystal, which is expected to display well-defined peaks in the diffraction patterns, whereas in amorphous materials, such as soft tissue and water, naturally broad peaks are obtained. The following relation is suitable for MB evaluation of these materials:

$$MB = \frac{(FWHM_m - FWHM_r)}{FWHM_r} \quad (14)$$

where $FWHM_m$ and $FWHM_r$ are the full-width at half-maximum of the main peak of the measured and reference diffraction patterns, respectively. In the current study, the diffraction pattern values introduced by Narten (1970) were used as reference for water. These data have been collected by a special diffractometer and used as gold standard in other studies (LeClair et al., 2006; Tartari et al., 2001).

2.2.6. Determining optimum values for different parameters for increasing sensitivity

After the relations between different parameters and resultant spatial and momentum transfer resolution and sensitivity were derived; determining of optimum values for each parameter (the sensitivity was as high as possible) was difficult because in the

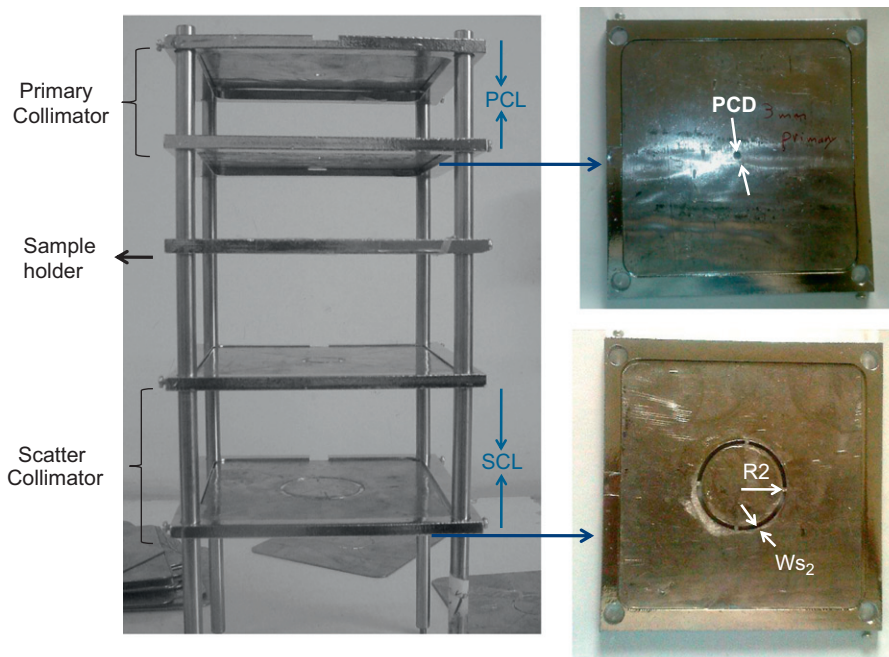


Fig. 3. Picture of planned and built flexible system consisting of primary and scatter collimators and a sample holder.

most situations, the sensitivity is reciprocal to the spatial and momentum transfer resolution. Therefore improvement of the system sensitivity is accompanied by a reduction of the spatial and momentum transfer resolution. It is clear that it is not permissible to increase sensitivity and reduce the measurement time at the cost of a reduction of spatial and momentum transfer resolution, as it makes differentiating tissue types by diffraction more difficult. Therefore, we have to determine the acceptable level of spatial and momentum transfer resolution based on the type of tissue studied and expectations from the system.

3. Results

3.1. Results of the relationship between spatial resolution and system parameters

The influence of different system parameters on horizontal spatial resolution was investigated using relation (4). From Fig. 4a, it is clear that an increase in PCD leads to an increase in HROI; thus decreasing horizontal spatial resolution. Enhancement of PCL leads to a decrease in the HROI (i.e. improvement of horizontal spatial resolution) (Fig. 4b).

Conversely increasing the SSD leads to an increase in the HROI, and consequent decrease of spatial resolution (Fig. 4c).

The influence of different parameters on vertical spatial resolution was investigated with respect to relation (5). Fig. 5a shows how the VROI is decreased as SCL is increased (i.e. the improvement of vertical spatial resolution) while the W_s is kept fixed (0.5 mm).

Of course, at a given angle and fixed W_s , the scatter collimator length is changed by variations of the radii of the scatter collimator diaphragms (R_1 , R_2). The size of radius of the lower diaphragm (R_2) is dependent on the radius of the active crystal of the detector. In this study the radius of the active crystal was 22 mm thus taking into account the gap between collimator and active crystal, the size of R_2 was determined to be 18 mm. Therefore, in equal circumstances, SCL is dependent on the size of the radius of the upper diaphragm (R_1).

In order to study the influence of W_{s2} and W_{s1} on system characteristics, they are considered to be equal (W_s) for simplicity. Of course, acquired relations have the ability to study W_{s2} and W_{s1} separately. An increase in the width of the scatter collimator diaphragms leads to an increase in the VROI (i.e. reduction of vertical spatial resolution) while the SCL is kept fixed (82 mm) (Fig. 5b).

3.2. Results of the relationship between momentum transfer resolution and system parameters

Using the relationships 6–10 and experimental tests; it was shown that when SCL is increased, the momentum transfer resolution is improved or momentum transfer blurring is decreased (Fig. 6a and 7). In contrast, an increase in the W_s leads to an increase in momentum transfer blurring, i.e. the reduction of momentum transfer resolution (Fig. 6b and Fig. 8).

3.3. Results of the relationship between sensitivity and system parameters

The influence of different parameters on the sensitivity was studied according to Eq. (11) and their accuracy was validated by experimental tests. From Fig. 9a it is clear that an increase in PCD leads to an increase in the relative peak height that is due to the enhancement of the volume of scattering because more scattered

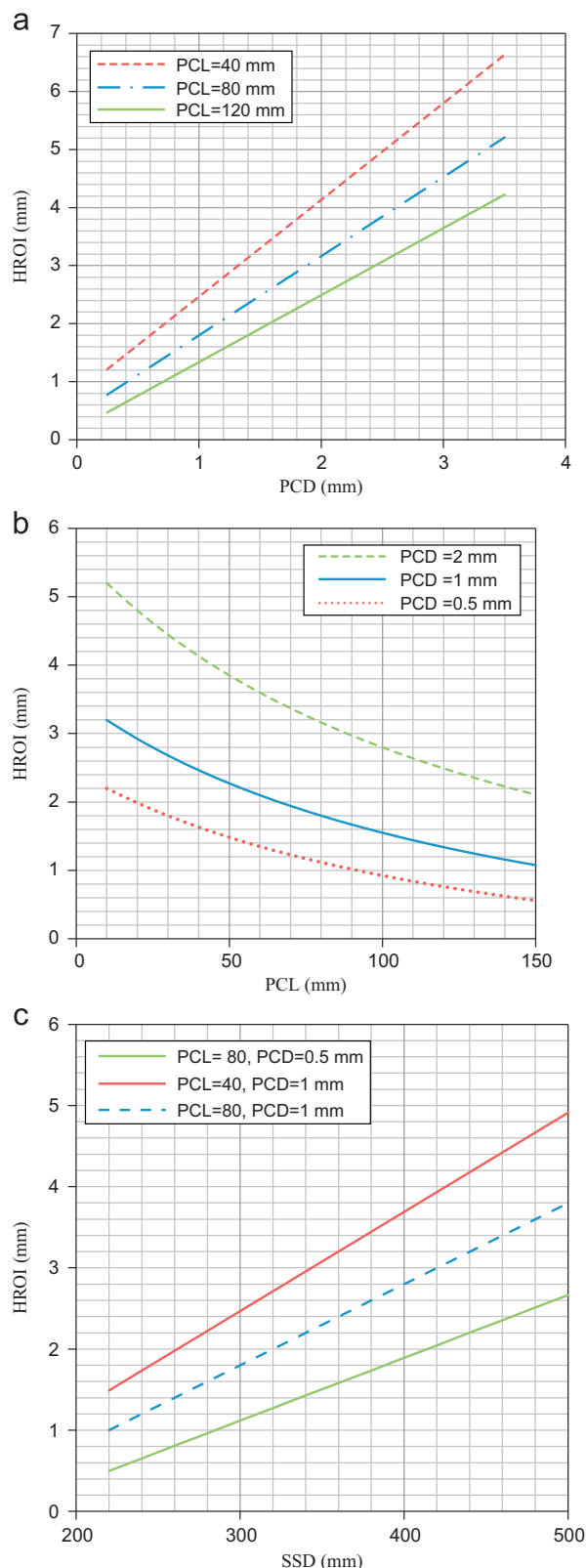


Fig. 4. The horizontal dimension of region of interest (HROI) as a measure of horizontal spatial resolution is influenced by variation of (a) primary collimator diameter (PCD), (b) primary collimator length (PCL) and (c) source to sample distance (SSD).

photons are produced and therefore the sensitivity is increased. Increasing PCL leads to a decrease in volume of the scattering tissue, therefore sensitivity is decreasing (Fig. 9b).

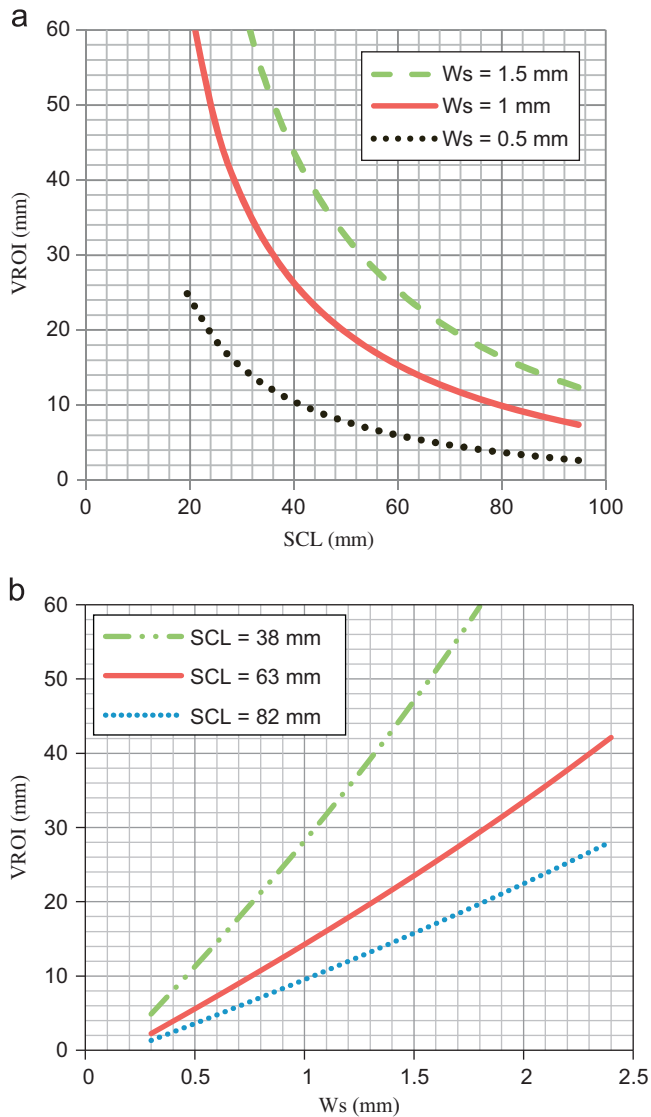


Fig. 5. The vertical dimension of region of interest (VROI) as a measure of vertical spatial resolution is influenced by variation of (a) scatter collimator length (SCL) and (b) slit width of scatter collimator diaphragms (W_s).

The relation between the variation of SSD and sensitivity is relatively complicated. Although by increasing SSD, the volume of scattering tissue increases and this leads to improvement in the scatter intensity (i.e. increasing of sensitivity), but on the other hand corresponding with the inverse square law, the intensity of the primary beam is decreasing so the intensity of scatter photons is decreasing that leading to a decrease of sensitivity. If the primary collimator is fixed then the two mentioned effects will neutralize each other, hence with changing of SSD, the sensitivity does not change.

With an increase of SCL, the volume of scattering is decreased and thus the sensitivity is decreased (Fig. 10a and Fig. 7). Unlike an increase in the W_s leading to an increase of sensitivity since more scattered photons can reach the detector (Fig. 10b and Fig. 8).

3.4. Results of the relationship between scatter angle (θ) and incident photon energy

The optimum scattering angle enabling the complete diffraction pattern of water was found. Since a range of momentum

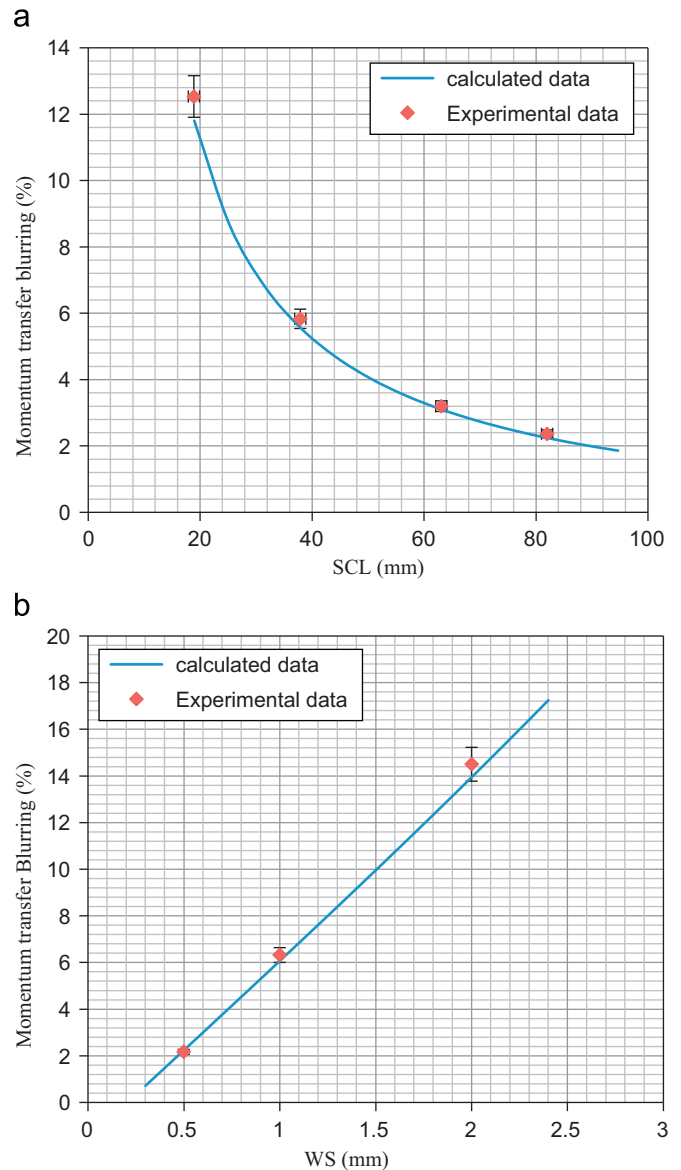


Fig. 6. The momentum transfer blurring as a measure of momentum transfer resolution is influenced by variation of (a) scatter collimator length (SCL) and (b) slit width of scatter collimator diaphragms (W_s).

transfer up to 3.17 nm^{-1} needs to be covered by the diffraction pattern of water, corresponding to Eq. (13), Table 1 shows optimum scatter angles for different energies, E (kVp). For example the best scattering angle was found to be at 9° , for the current use the tube energy was 50 kVp.

As shown in Fig. 11, using a smaller angle may lead to a partial diffraction pattern, which has missing information at higher momentum transfer values.

3.5. Optimum values for different parameters in favor of increasing the sensitivity

Using the results from previous sections, as an example, optimum parameters were determined for obtaining the diffraction patterns of healthy and cancerous breast tissues while the measurement time was kept as low as possible. It was done by considering acceptable levels of spatial and momentum transfer resolutions (Table 2).

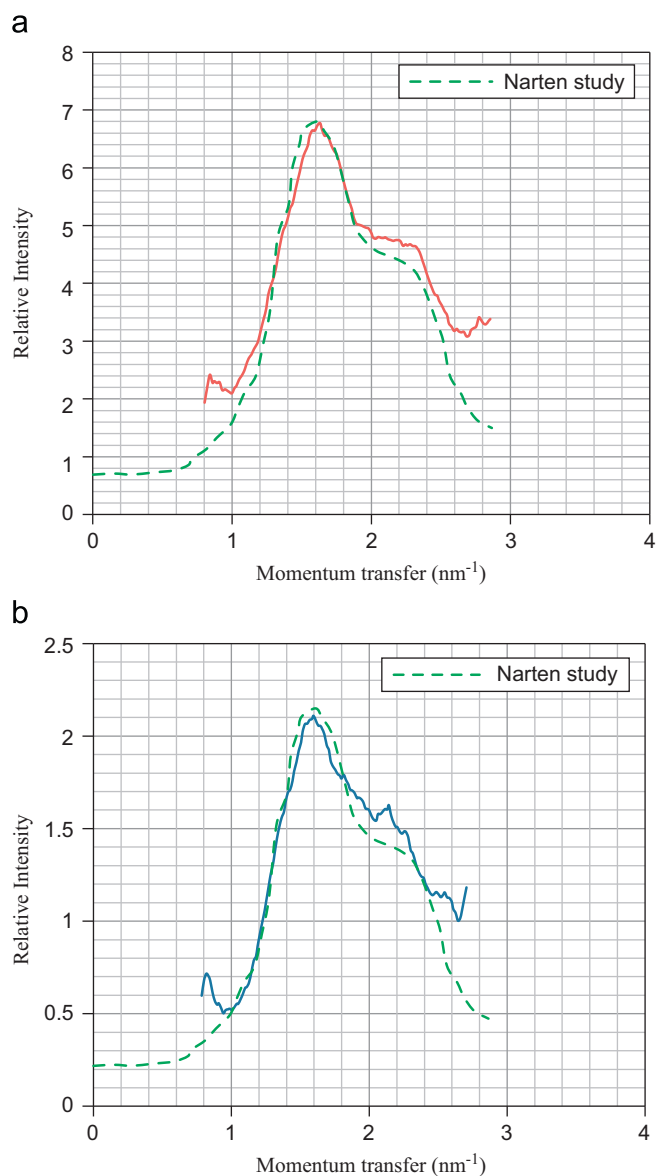


Fig. 7. Diffraction patterns of water obtained experimentally at scatter angle (θ) equal to 9° and $W_s=0.5$ mm for two different values of scatter collimator length (SCL): (a) SCL=38 mm that induces MB=5.83% and (b) SCL=82 mm that induces MB=2.37%.

As mentioned in Section 2.2.6 the relations between different parameters and resultant spatial and momentum transfer resolution and sensitivity were derived; but determining of optimum values for each parameter was difficult because in most situations, the sensitivity is reciprocal to the spatial and momentum transfer resolution. Therefore, we have to determine the acceptable level of spatial and momentum transfer resolution based on the type of tissue studied and expectations from the system. In the following we explain how to determine the optimum or suitable value for each parameter.

In the first step, the optimum scattering angle was determined according to Eq. (13). In the second step, the acceptable level of momentum transfer resolution as determined in this study was 5% for biological tissues, which was similar to previous studies (Poletti et al., 2004; Harding et al., 1990). Then the acceptable level of VROI was determined using Eqs. (6)–(10). After inserting the corresponding values in the Eq. (5), appropriate values for W_s and SCL could be obtained, noting that the remainder parameters

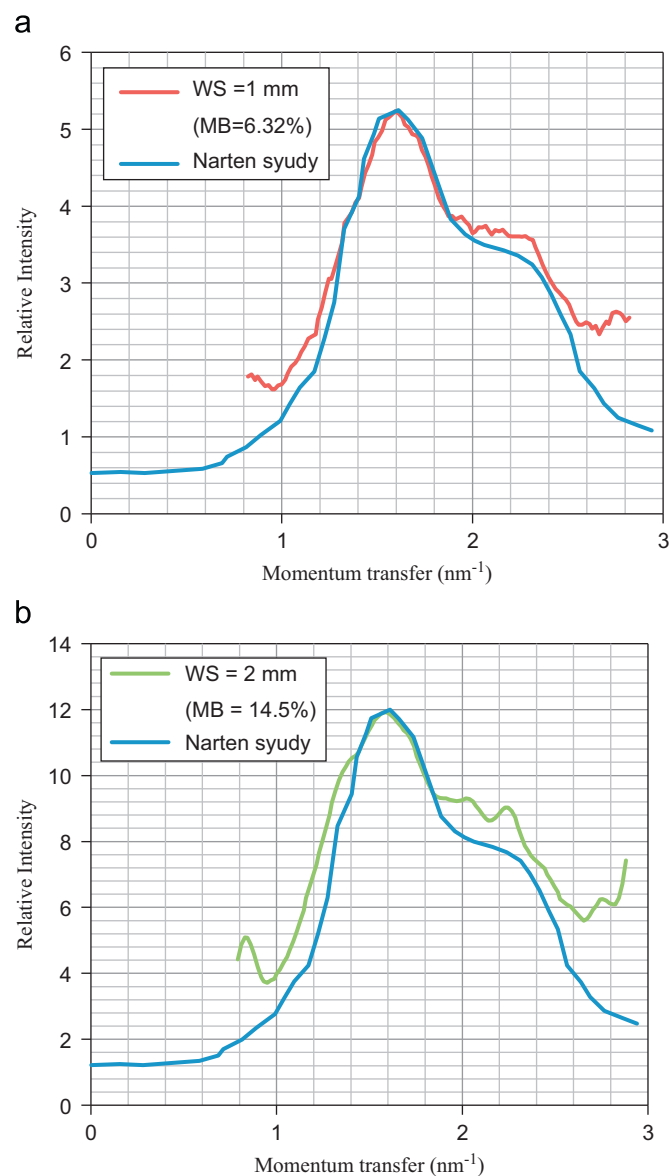


Fig. 8. Diffraction patterns of water obtained experimentally at scatter angle (θ) equal to 9° and SCL=82 mm for two different values of slit width of scatter collimator diaphragms (W_s): (a) $W_s=1$ mm that induces MB=6.32% and (b) $W_s=2$ mm that induces MB=14.5%.

are fixed in each system (In our system $LT=1.5$ mm, $R_2=18$ mm and $\theta=9^\circ$). A variety of W_s and SCL sizes could be selected for obtaining a certain size of VROI. However it was preferable to keep SCL constant to be 82 mm because contamination from primary photons was created due to longer SCL i.e. smaller R_1 in a fixed angle. Then the acceptable level of the vertical spatial and momentum transfer resolutions could be obtained by changing of W_s exclusively. For example in order to provide momentum transfer resolution to be 5% and then the vertical spatial resolution (VROI) to be 10 mm the size of W_s was calculated to be 0.85 mm.

The acceptable level of HROI as a criterion of horizontal spatial resolution was also determined to be 2 mm, which is suitable for clinical application in comparison with other imaging systems such as SPECT or PET. After inserting the related values in Eq. (4), appropriate values for PCD and PCL could be obtained, taking into consideration that the remainder parameters are fixed in each system (in our system $\alpha=1.2$ mm, SAD=140 mm and SSD was

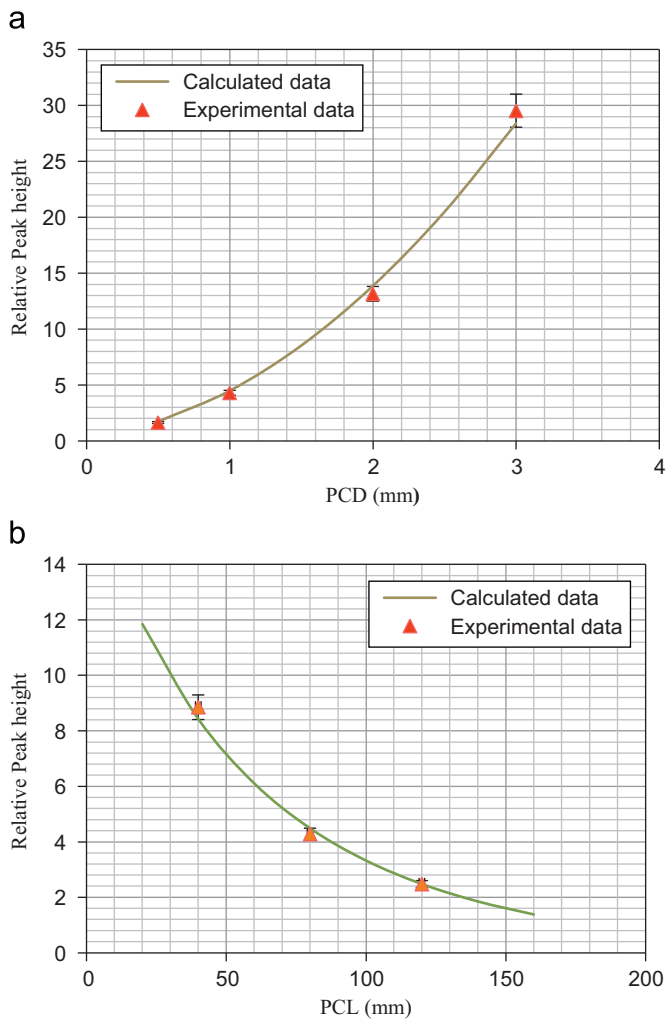


Fig. 9. The relative peak height as a measure of sensitivity is influenced by variation of (a) primary collimator diameter (PCD) and (b) primary collimator length (PCL).

kept constant to be 300 mm that is suitable for clinical application). A variety of PCD and PCL sizes could be selected for obtaining a certain size of HROI. However it was preferable to keep PCD constant to be 1 mm because alignment of the smaller PCD was hard. Then the acceptable levels of the horizontal spatial resolution could be obtained by changing of PCL exclusively. For example in order to provide the horizontal spatial resolution to be 2 mm the size of PCL was calculated to be 80 mm.

In this example, considering optimum parameters, the required measurement time for obtaining diffraction patterns of breast tissue was found to be in the order of 20–30 s.

4. Discussion

The aim of our study was to define the relationship between various parameters of an EDXRD system and some performance specifications such as sensitivity, spatial resolution and momentum transfer resolution. Since there was usually a trade-off between these resolutions and sensitivity, the acceptable levels of spatial resolution and momentum transfer resolution were defined. Then as an example, we determined the optimal parameters for an increase in sensitivity i.e. decrease of measurement time for obtaining the diffraction pattern of breast tissues.

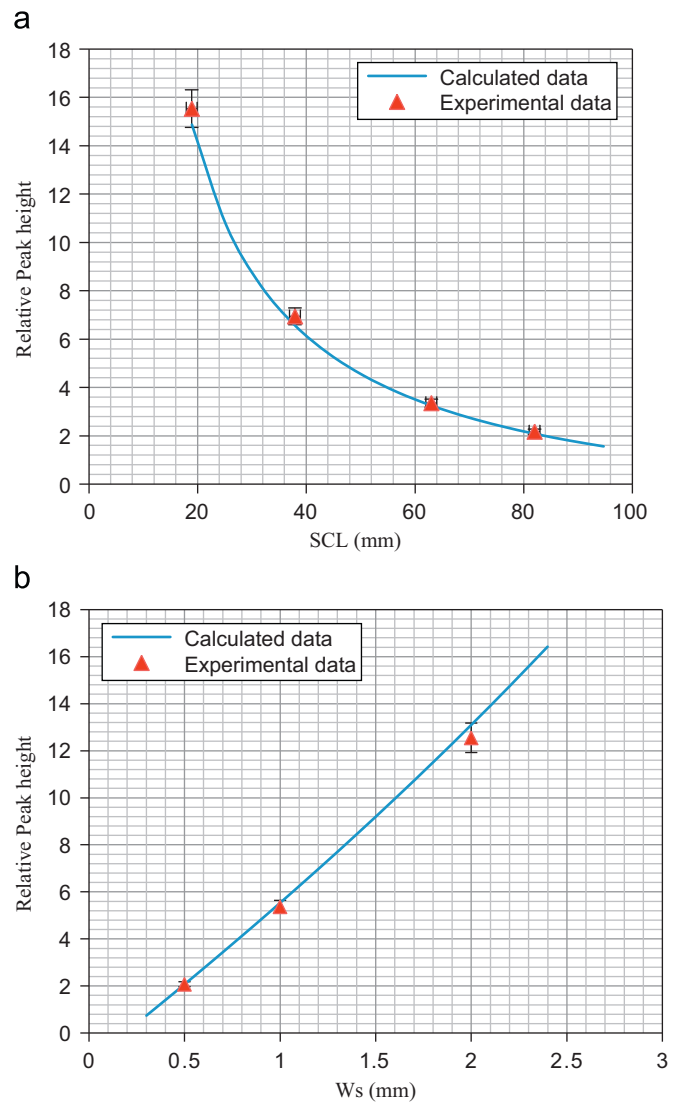


Fig. 10. The relative peak height as a measure of sensitivity is influenced by variation of (a) scatter collimator diameter (SCL) and (b) slit width of scatter collimator diaphragms (W_s).

Table 1

Optimum angle for different energies for obtaining diffraction patterns of water.

Energy (kVp)	Optimum scatter angle
30	15.0
35	12.9
40	11.3
45	10.0
50	9.0
55	8.2
60	7.5
70	6.4
75	6.0
80	5.6
85	5.3
90	5.0
95	4.7
100	4.5

The acceptable level of momentum transfer resolution as determined in this study was 5% for breast tissues which was similar to previous studies (Poletti et al., 2004). We considered the

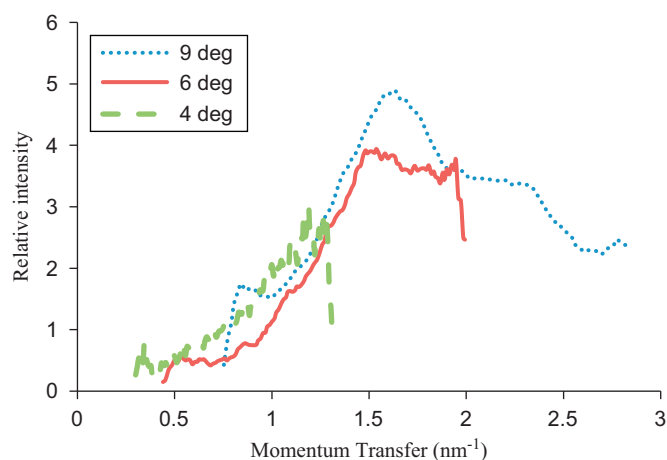


Fig. 11. Comparison of three diffraction patterns of water obtained with three different angles.

Table 2

Optimum parameters for obtaining diffraction pattern of breast tissue with the acceptable level of 5% for momentum transfer resolution and the acceptable levels for vertical and horizontal spatial resolution to be less than 10 and 2 mm, respectively.

Parameter	Optimum value
Primary collimator diameter (PCD)	Optimum value
Primary collimator length (PCL)	1 mm
Source to sample distance (SSD)	300 mm
Optimum scatter angle for energy 50 kVp	9°
Width of upper diaphragm (Ws ₁)	0.85 mm
Width of lower diaphragm (Ws ₂)	0.85 mm
Scatter collimator length (SCL)	82 mm

acceptable levels of VROI and HROI (as vertical and horizontal spatial resolutions), which for clinical application need to be less than 10 and 2 mm, respectively.

Primary collimator parameters including PCL and PCD were selected according to Eq. (4) and the acceptable level of horizontal spatial resolution for maximizing the sensitivity. Accordingly defining PCL and PCD size of 1 mm and 80 mm, respectively, improved the sensitivity only in this case two times comparing a PCL size of 150 mm as proposed by Changizi et al. (2005) and Changizi et al., (2008).

The SSD should be chosen as low as possible because it induces improvement of horizontal spatial resolution by considering Eq. (4) and Fig. 4c and also enhancement of sensitivity according to inverse square law. Therefore, with regard to the SCD and PCL sizes, we set SSD to a size of 300 mm.

The scatter collimator parameters such as SCL and Ws should be set according to relation 5–10 and Fig. 5 and the acceptable level of momentum transfer resolution. Considering an SCL size of 82 mm and Ws size of 0.85 mm through this study was suitable enough to provide acceptable resolutions while the sensitivity or measurement time was practically valid. Of course there are other options for SCL and Ws, which can satisfy the same acceptable resolutions, for example SCL size of 42 mm and Ws size of 0.5 mm.

According to this study, the optimum value for the scattering angle was determined to be 9° for a source energy of 50 kVp. LeClair et al. (2006) showed this scattering angle to be optimum for obtaining diffraction patterns of both water and breast tissues. They obtained this optimum value by means of experimental tests.

Bomsdorf et al., 2004 used a simulation program for EDXRD system optimization but learning of their method is necessary for performance in other applications especially for non-crystalline materials (e.g. water and biological tissues) that solution of this problem is difficult and time-consuming. While, using derived relations and curves in our study can simply be incorporated for optimization of other applications.

5. Conclusion

In this study, the relations between various parameters of an EDXRD system and some performance specifications such as sensitivity, spatial resolution and momentum transfer resolution were extracted. As an example of optimization, the optimum parameters were determined for obtaining diffraction patterns of the breast tissue for an efficient measurement time. The applied method in this study allows the comparison of the sensitivity in different situations to perform an efficient measurement. It also provides useful information regarding the spatial resolution and momentum transfer resolution in each case. Consequently, the different protocols corresponding to the various choices of setting parameters can be easily compared. A first result is that an unsuitable choice of the setting parameters can decrease the sensitivity i.e. increase the measurement time. Second, this study introduces a useful tool for EDXRD optimization in applications other than the breast cancer detection.

Acknowledgment

This work was supported by Tehran University of Medical Sciences, Tehran, Iran.

References

- Bomsdorf, H., Muller, T., Strecker, H., 2004. Quantitative simulation of coherent X-ray scatter measurements on bulk objects. *J. X-ray Sci. Technol.* 12, 83–96.
- Cunha, D.M., Oliveira, O.R., Perez, C.A., Poletti, M.E., 2006. X-ray scattering profiles of some normal and malignant human breast tissues. *X-ray Spectrom.* 35, 370–374.
- Chaparian, A., Oghabian, M.A., Changizi, V., 2009. Obtaining molecular interference functions of X-ray coherent scattering for breast tissues by combination of simulation and experimental methods WC 2009. In: *IFMBE Proceedings* 25/IV, 2009, pp. 1736–1739.
- Changizi, V., Oghabian, M.A., Speller, R., Sarkar, S., Kheradmand, A.A., 2005. Application of small angle X-ray scattering (SAXS) for differentiation between normal and cancerous breast tissue. *Int. J. Med. Sci.* 2, 118–121.
- Changizi, V., Arab Kheradmand, A., Oghabian, M.A., 2008. Application of small angle X-ray scattering (SAXS) for differentiation among breast tumors. *J. Med. Phys.* 33, 19–23.
- Farquharson, M.J., Geraki, K., 2004. The use of combined trace element XRF and EDXRD data as histopathology tool using a multivariate analysis approach in characterising breast tissue. *X-ray Spectrom.* 33, 240–245.
- Harding, G., Newton, M., Kozanetzky, J., 1990. Energy-dispersive X-ray diffraction tomography. *Phys. Med. Biol.* 35, 33–41.
- Kidane, G., Speller, R.D., Royle, G.J., Hanby, A.M., 1999. X-ray scatter signatures for normal and neoplastic breast tissues. *Phys. Med. Biol.* 44, 1791–1802.
- LeClair, R.J., Boileau, M.M., Wang, Y., 2006. A semianalytical model to derive differential linear scattering coefficients of breast tissue from energy dispersive X-ray diffraction measurements. *Med. Phys.* 33, 959–965.
- Narten, A.H., X-ray diffraction data on liquid water in the temperature range 4–200 °C. Oak Ridge National Laboratory Report No. ORNL 4578, 1970.
- Poletti, M.E., Gonçalves, O.D., Mazzaro, I., 2002. X-ray Spectrom. 31, 57.
- Poletti, M.E., Gonçalves, O.D., Mazzaro, I., 2004. Measurements of X-ray scatter signatures for some tissue-equivalent materials. *Nucl. Instrum. Methods Phys. Res. B* 213, 595–598.
- Speller, R.D., 1999. *X-ray Spectrom.* 28, 244.
- Theodorakou, C., Farquharson, M.J., 2008. Human soft tissue analysis using X-ray or gamma-ray techniques. *Phys. Med. Biol.* 53 (11), 111–149.
- Tartari, A., Taibi, A., Bonifazzi, C., Baraldi, C., 2001. Updating of form factor tabulations for coherent scattering of photons in tissues. *Phys. Med. Biol.* 47, 163–175.